Materials Science & Engineering A 591 (2014) 59–68

Contents lists available at ScienceDirect

Materials Science & Engineering A

journal homepage: www.elsevier.com/locate/msea

Cyclic deformation and fatigue behaviors of Hadfield manganese steel

J. Kang [a], F.C. Zhang [a,*], X.Y. Long [a], B. Lv [b]

[a] State Key Laboratory of Metastable Materials Science and Technology, Yanshan University, Qinhuangdao 066004, China
[b] School of Environmental and Chemical Engineering, Yanshan University, Qinhuangdao 066004, China

ARTICLE INFO

Article history:
Received 22 June 2013
Received in revised form
27 September 2013
Accepted 23 October 2013
Available online 31 October 2013

Keywords:
Low cycle fatigue
High cycle fatigue
Cyclic deformation
Internal stress
Effective stress
Hadfield manganese steel

ABSTRACT

The cyclic deformation characteristics and fatigue behaviors of Hadfield manganese steel have been investigated by means of its ability to memorize strain and stress history. Detailed studies were performed on the strain-controlled low cycle fatigue (LCF) and stress-controlled high cycle fatigue (HCF). Initial cyclic hardening to saturation or peak stress followed by softening to fracture occurred in LCF. Internal stress made the dominant contribution to the fatigue crack propagation until failure. Effective stress evolution revealed the existence of C–Mn clusters with short-range ordering in Hadfield manganese steel and demonstrated that the interaction between C atoms in the C–Mn cluster and dislocation was essential for its cyclic hardening. The developing/developed dislocation cells and stacking faults were the main cyclic deformation microstructures on the fractured sample surface in LCF and HCF, which manifested that fatigue failure behavior of Hadfield manganese steel was induced by plastic deformation during strain-controlled or stress-controlled testing.

1. Introduction

Hadfield manganese steel has attracted widespread concern and interest owing to its excellent work hardening and wear-resistance, which has resulted in a significant quantity of work being published in the literature and Hadfield steel becoming the traditional material to be used in railway crossings [1–6]. When the train wheel passes, the railway crossing suffers different types of deformation. In view of cyclic stress, the high cycle fatigue (HCF) dominated by elastic strain occurs in terms of the whole of the railway crossing, whereas low cycle fatigue (LCF) is dominated by plastic strain occurring on the work surface of the railway crossing. An analysis of cyclic deformation under different strain amplitudes in Hadfield manganese steel can contribute to a deeper and more thorough understanding of the fatigue fracture mechanisms as well as to improvements in the design and application of railway crossings.

However, investigations associated with fatigue properties of Hadfield manganese steel have focused mainly on rolling contact fatigue, with little attention given to LCF. Harzallah [7] carefully studied the influence of different contact parameters on the contact rolling fatigue behavior of Hadfield manganese steel. Lv [8] analyzed the reasons for failure using samples from a Hadfield manganese steel crossing and thought that the initial contact rolling fatigue cracks were caused by the high concentration of vacancy clusters in the subsurface layer of the Hadfield manganese steel crossing. Schilke [9] studied the LCF behavior of Hadfield manganese steel in rolled and in as-cast conditions and found that the cyclic stress response of fatigue failure was initially cyclic hardening, followed by softening to fracture. An investigation of the cyclic deformation behavior in 316L austenitic stainless steel also showed a cyclic hardening in the early period, followed by softening to failure fracture. Owing to its low stacking fault energy (SFE), the planar slip resulted in dislocation tangles arranged originally in thin sheets parallel to the primary slip plane, separated by dislocation-free sheets in 316L austenitic stainless steel [10,11]. However, Hadfield manganese steel possesses a higher SFE ($\sim$50 mJ/m^2) compared with those of austenitic stainless steels ($\sim$20 mJ/m^2). The high strain hardening capacity of Hadfield manganese steel results primarily from the deformed twinning [12–14] and reorientation of C atoms in C–Mn clusters in the cores of dislocations [2,3,15] in tensile or compression tests. However, the cyclic deformation behaviors and mechanisms of Hadfield manganese steel are not clear at present.

In this paper, the cyclic deformation characteristics and fatigue behaviors of Hadfield manganese steel are studied and discussed with respect to LCF and HCF. Detailed studies were performed on the cyclic stress response, fatigue life, internal stress, and effective stress partitioning from the hysteresis loop and hardness distribution, linked with the deformation and fracture microstructures during cyclic straining and stressing.

2. Experimental materials and procedures

2.1. Material and tensile testing

The studied material, traditional Hadfield manganese steel, contains 12.0 wt% Mn and 1.2 wt% C. The plate material was

* Corresponding author. Tel.: +86 335 8063949; fax: +86 335 8074568.
E-mail address: zfc@ysu.edu.cn (F.C. Zhang).

0921-5093/$ - see front matter © 2013 Elsevier B.V. All rights reserved.
http://dx.doi.org/10.1016/j.msea.2013.10.072

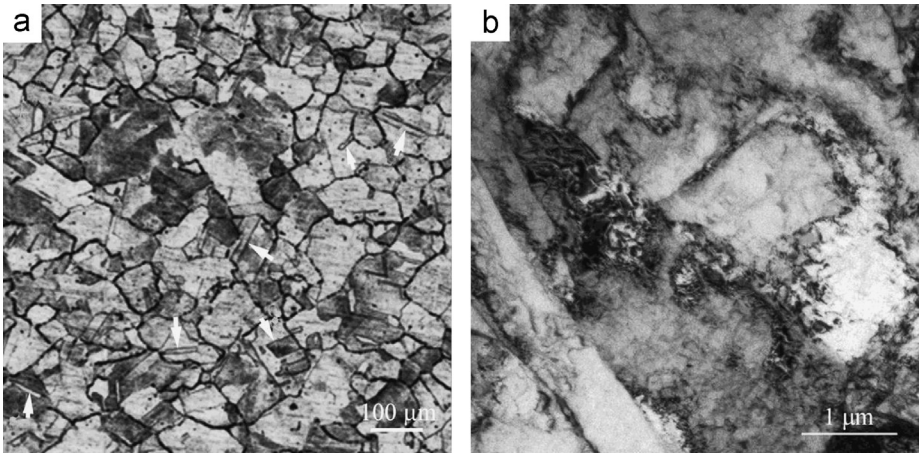

Fig. 1. OM (a) and TEM (b) microstructures of Hadfield manganese steel after water quenching.

supplied in forged condition, 25 mm thick × 45 mm high. A single austenitic phase was obtained by annealing at 1050 °C for 0.5 h, followed by quenching, as shown in Fig. 1a. A quenching twinning boundary (indicated by the white arrow in Fig. 1a) and a certain density of dislocation with planar net and free were present in Fig. 1b.

Monotonic tensile testing was performed on plate samples with 10 mm gauges and 3 mm thickness, and the tested axial direction was parallel to the forging direction. A strain rate of 4×10^{-3} s^{-1} was selected.

2.2. Fatigue testing

Three-point bending fatigue tests in the high cycle regimes were carried out on a QB-100 kN high frequency fatigue testing machine. The experiments were controlled by stress with a 0.1 load ratio and 80 Hz frequency. A configuration of the three-point bending fatigue samples with dimensions of $10 \times 10 \times 65$ mm^3 and a span gauge of 45 mm was adopted. The bending fatigue strength was obtained according to the following equation:

$$\sigma = \frac{3PL}{2BH^2} \tag{1}$$

where σ and P represent the maximum stress and load on the sample surface, and L, B and H stand for the span gauge, width and height of the samples, respectively.

The bending fatigue testing was carried out until fracture of the specimen or 10^7 cycles according to a Chinese Test Standard: GB 3075-82. In order to obtain a stable stress condition, the bending fatigue was performed with a continuous increase of the stress level until reaching the stabilized setting stress. The increased amplitude of stress level for every sample was kept constant and the adjustment period of increasing stress was usually within 5×10^3 cycles. The bending fatigue strength, $\sigma_{0.1bending}$, and S–N curves were obtained by the up-and-down and group methods, respectively. The number of specimens in the up-and-down method usually needs to be more than 13. Three to five stress levels are applied while the stress increment $\Delta\sigma$ is within 5% of the predicted $\sigma_{0.1bending}$. The first stress should be slightly higher than the predicted $\sigma_{0.1bending}$. The stress applied later increases or reduces according to the result of the previous sample (success or failure) until the fatigue test is finished. If a pair of opposite results appears for the first time within the range of stress fluctuation values, this pair of data can be judged by the effective data to be utilized. The equation for calculating $\sigma_{0.1bending}$ can be expressed as

$$\sigma_{0.1bending} = \frac{1}{m}\sum_{i=1}^{n} V_i\sigma_i \tag{2}$$

where m is the total effective times of fatigue testing including the data points of success and failure, n is the test stress level series, σ_i and V_i are the i levels of stress and the number of testing under i levels of stress, respectively.

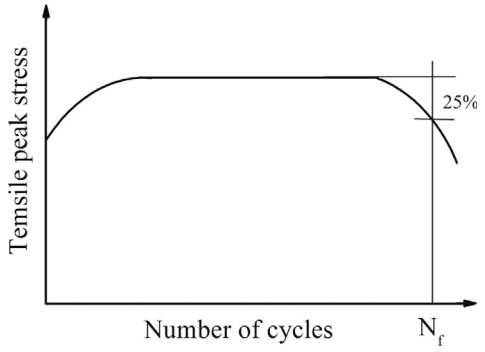

Fig. 2. End-of-test criterion based on stress for materials with stable behavior after initial hardening and then softening.

Different maximum stresses (σ_{max}) with decreasing values were applied as the higher stress section (limited fatigue life) in S–N curves. There were more than two samples under each σ_{max} to ensure the validity of the data.

The LCF test was conducted on an MTS servohydraulic fatigue-testing machine. The fatigue test was done according to the Chinese Test Standard GB 15248-2008. Plate samples with 10 mm gauges and 3 mm thickness were also adopted and the tested axial direction was parallel to the forging direction. The tested plates were ground and polished with silicon carbide paper down to 0.1 μm along the longitudinal direction. The strain-controlled test had a mean zero strain ($R=-1$) at a strain rate of 4×10^{-3} s^{-1}. Total strain amplitudes of 3×10^{-3}, 4×10^{-3}, 6×10^{-3}, 8×10^{-3}, and 1×10^{-2} were selected. The fatigue failure was judged as the cycle number when the tensile peak stress decreased to a value approximately 25% below the plateau stress. Fig. 2 presents a schematic drawing of the end-of-test criterion based on stress.

There are three main accepted methods of calculating the internal stress and effective stress extracted from the hysteresis loop: (i) the original Cottrell method [16]; (ii) the density functional theory of critical internal stress proposed by Polák [17]; and (iii) the Handifield–Dickson method based on the Cottrell